CHAPTER 31

KINEMATICS AND RETURN FLOW IN A CLOSED WAVE FLUME

Jerald D. Ramsden[1] , AM. ASCE
John H. Nath[2] , F. ASCE

ABSTRACT

Stokes (1847) showed that finite amplitude progressing waves cause a net drift of fluid, in the direction of wave motion, which occurs in the upper portion of the water column. In a closed wave flume this drift must be accompanied by a return flow toward the wave generator to satisfy the conservation of mass. This study presents Eulerian velocity and water surface measurements soon after the onset of wave motion from 12 locations in a large scale flume. Waves with $.67 \leq kh \leq 2.29$ and $.09 \leq H/h \leq .39$ were produced in a water depth of 3.5 meters. Superimposing the return flow theory of Kim (1984) with seventh order stream function theory is shown to improve the velocity predictions. The measured return flows are a function of time and depth and agree with Kim's theory as a first approximation. The mean water surface set-down agrees with the theory of Brevik (1979) except for the nearly deep water waves.

INTRODUCTION

Periodic progressing gravity waves confined in a closed wave flume cause a longitudinal circulation to develop. This circulation is driven by mass transport [Stokes (1847)] in the direction of wave propagation and results in a return flow toward the wave generator. The circulation in closed flumes has been extensively studied

[1]Graduate Student, W. M. Keck Laboratory, California Institute of Technology. Pasadena, CA

[2]Professor Emeritus, Department of Civil Engineering, Oregon State University. Corvallis, OR.

in Lagrangian coordinates while few Eulerian measurements have been published. Many studies of the Eulerian water particle velocities and wave force measurements on fixed structures are carried out in closed wave flumes. Measurements from these studies will include the effects of the circulation. The free waves, beach reflections, wind, flume geometry, and the initial conditions may also differ between the wave flume and the ocean.

Studies in flumes are often conducted within a few or several waves after the onset of wave motion to minimize reflections and oscillations characteristic of the flume geometry. The objective of this study is to characterize the behavior of the return flow during this time period.

Two distinct methods have been used to predict the return flow. In one method, inviscid wave theory is used to compute a volume flux due to mass transport. Then a steady uniform return flow (R_c) is superimposed on the wave theory, such that the volume flux due to the return flow cancels the flux from the mass transport. This method was used on stream function wave theory by Dalrymple (1976) and on Stokes' second through fifth order wave theories by Kim (1984). The other was pioneered by Longuet-Higgins (1953) who solved the 'conduction equation' assuming a viscous fluid. He obtained an explicit solution for the circulation in a closed two dimensional flume. The conduction solution predicts parabolic return flow profiles over depth in contrast to the uniform return flow assumed with the inviscid theory. Return flows predicted from inviscid theory should provide reasonable results for flow outside the boundary layers during the first several waves as discussed by Longuet-Higgins (1953) and as shown in this paper. Longuet-Higgins' method provides reasonable predictions near the bottom boundary layer [Russel and Osorio (1958)] and throughout the water column when the wave motion has continued for several hundred wave periods [Bullock and Short (1985)].

To the authors' knowledge only Nath (1978) and Kim (1984) have published Eulerian return flow measurements which were collected soon after the start of wave motion. Both of these authors used the same flume, water depth, and approximately the same wave conditions as used in this study. Both their results contained considerable variability. Due to this variability, Kim found that Longuet-Higgins method and the one developed by him based on

Stokes fifth order wave theory yeild similar errors when compared with both their measurements.

THEORY

As discussed by Longuet-Higgins (1953), when the wave motion starts, the flow is everywhere irrotational except in the boundary layers along the flume walls, the bottom, and the free surface. The boundary layer thickness δ along the flume bottom is approximately $(2\nu/\omega)^{1/2}$, where ω is the angular frequency of the wave motion and ν is the kinematic viscosity of water. For the conditions of this study, δ is on the order of a few millimeters. If the boundary layer thickness on the sides and surface is of this same order, then approximately two tenths of one percent of the flume cross section lies within the boundary layers. Thus, inviscid wave theory should adequately predict the mass transport volume flux and the return flow within the first several wave periods.

The results of Kim's (1984) return current model [see also Kim, Hudspeth, and Sulisz (1986)] based on Stokes second and fifth order wave theories are presented in Figure 1, where T is the wave period, h the water depth, H the wave height, $L_o = gT^2/2\pi$ the deep water wave length where g is the gravitational constant, $C_o = L_o/T$ the deep water wave celerity, and R_c the theoretical return flow. His model, based on the assumption that the return flow is steady and uniform, is the first to include the contribution from the free waves. The fifth order return flow theory is used throughout this paper.

Kim, Hudspeth, and Sulisz (1986) showed that a complete second order solution of the wavemaker boundary value problem requires a time independent potential in addition to the Stokes wave, a free wave, and a series of evanescent waves which were treated earlier by others. The evanescent waves decay with distance from the wave generator and do not propagate. Figure 1 is only valid beyond 3 water depths from the wave generator where the evanescent waves have decayed to a negligible value. The free wave is forced at twice the wave generator frequency. Since the free wave obeys its own dispersion relation, it propagates slower than the Stokes wave which causes the waveform to be nonpermanent along the flume [Buhr Hansen and Svendsen (1974)].

In this study seventh order stream function wave theory is linearly superimposed with Kim's return flow theory. Studies by Chandler and Hinwood (1982) and Dalrymple (1976) indicate that

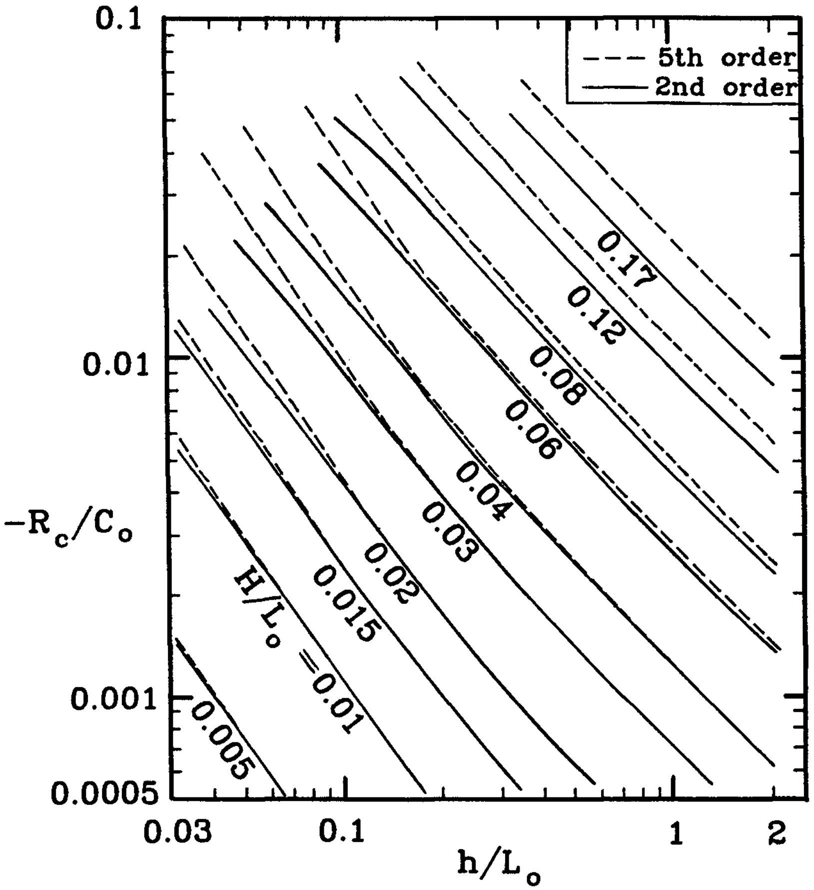

Figure 1: Return current in a closed wave flume for a flap type wavemaker computed from Stokes wave theory [adapted from Kim(1984)].

small currents, like those due to the return flow, can be linearly superimposed with wave theory since the nonlinear interaction effects are quite small.

From the concept of the radiation stress, Longuet-Higgins and Stewart (1964) showed that waves propagating into still water may cause a change in the mean water surface elevation. The mean water levels in this study are compared with a theory presented by Brevik (1979). He derived an expression for the water surface setdown under a packet of waves propagating in water of a constant depth. The wave packet was assumed to have a Gaussian wave height distribution in space and a narrow banded wave number spectrum.

EXPERIMENT

The wave kinematics were measured in the O. Howard Hinsdale Wave Research Laboratory wave flume (Fig. 2.) during February 1985. The flume is 3.94 m. wide, 96.5 m. long, and has walls of smooth concrete. The wave board is hinged at the flume bottom and driven in a sinusoidal motion by a hydraulic piston.

Four Marsh McBirney Model 711 current meters were used to measure the horizontal and vertical velocities. They operate on the principle of Faraday's law of electromagnetic induction. Each probe is a 2.5 cm. diameter cylinder with a length of 25 cm. and senses the velocities in a plane perpendicular to its axis. Over the frequency range of interest in this study, 0.0 to 2.0 Hz., the current meter electronics behave as a linear first order filter, Ramsden (1987). Both axes of each meter were calibrated using two independent methods which gave complimentary results.

The water particle velocities were measured in twelve locations for each wave condition. The water depth was 3.77 m at the test section during all the measurements. The 25 wave conditions were repeated three times with the meters in different arrangements. Figure 2 shows the three stations where the measurements were collected. Two current meters were placed on each side of the flume for arrangement no. 1 and no. 2. For meter arrangement no. 3 all the current meters were placed on the same side of the flume with two at station no. 1 and two at station no. 3. Three of the current meters were mounted .33 meters from the flume wall while the other was .98 meters from the wall. All the measurements were collected within $-.74 \leq z/h \leq -.04$, where z is the vertical coordinate with its origin at the water surface and directed positive upward.

The wave conditions were obtained by using five different wave generator strokes for each of five wave periods. The wave periods were 2.5, 3.7, 4.6, 5.3, and 6.0 seconds. The stroke was set to obtain wave heights ranging between .33 m. to the maximum possible height for each wave period. The maximum wave heights ranged from 1.07 meters at T=2.5 sec., up to 1.37 m. at T=3.7 sec., then down to .94 m. for the 6.0 sec. waves. The water surface profile (η) was measured with sonic wave profilers at the center of the flume

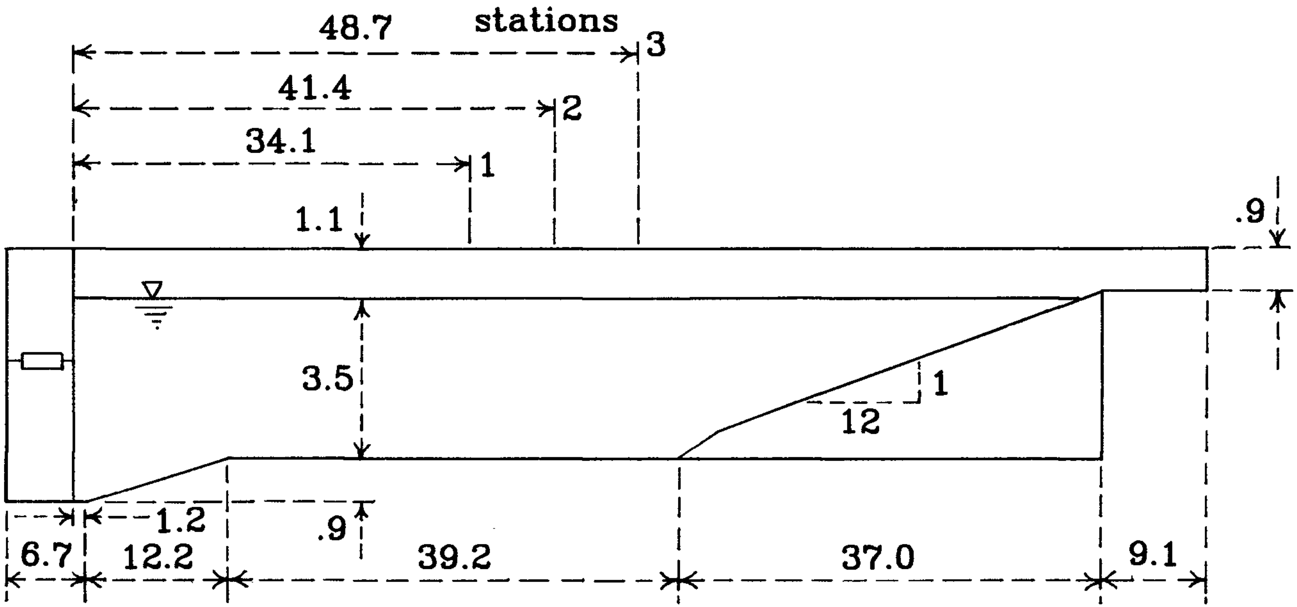

Figure 2: The wave flume at the O. Howard Hinsdale Wave Research Laboratory on the Oregon State University Campus (all dimensions are in meters).

in each cross section containing current meters. The measurements were collected for 14 wave periods beginning with the initial wave disturbance at the current meter locations. The data were recorded digitally at 256 samples per wave period. Before the wave generator was started, 256 samples were collected which are averaged to establish the still water level and the velocity reference. For some of the runs during the first current meter arrangement, an additional block of 14 wave periods of data was collected while letting the wave generator run continuously. This second data block began from 30 sec. to 120 sec. after the end of the first data block.

RESULTS

Out of 525 velocity records 439 were clean and consistent. For the other 86 records there were some problems which included very noisy or erratic reference measurements, voltage jumps during sampling, and some runs where one or two of the meters gave no response.

Figures 3a through 3c show a comparison of the horizontal velocity measurements vs. theory under the wave peak (positive velocities) and trough (negative velocities). Measurements from the maximum wave heights obtained at each wave period are shown. The questionable measurement in Fig. 3a is from a current meter that was intermittently submerged and gave quite low velocities, relative to the other measurements, for the 2.5 sec. waves. This may reveal a minimum amount of submergence time for the model 711 to record the actual velocity when placed above the wave trough. The questionable measurements in Figures 3b and 3c are from a current meter which was working intermittently.

Figure 3a shows velocity profiles at the crest and the trough of a fairly deep water wave. The data from this study and those from Kobune (1978) and Jensen (1978) agree quite well even though they were collected at widely different times and with different types of current meters. Jensen and Kobune used a water depth of 3.35 m. instead of the 3.50 m. of this study.

The measurements follow the theoretical trends quite well although there is some variability which tends to increase with the wave length. This variability is most likely due to both the free waves and the beach reflections. Nath measured the beach reflections with the same flume geometry in 1982. He found the reflection coefficient to be independent of the wave height and to range from a)

b)

c)

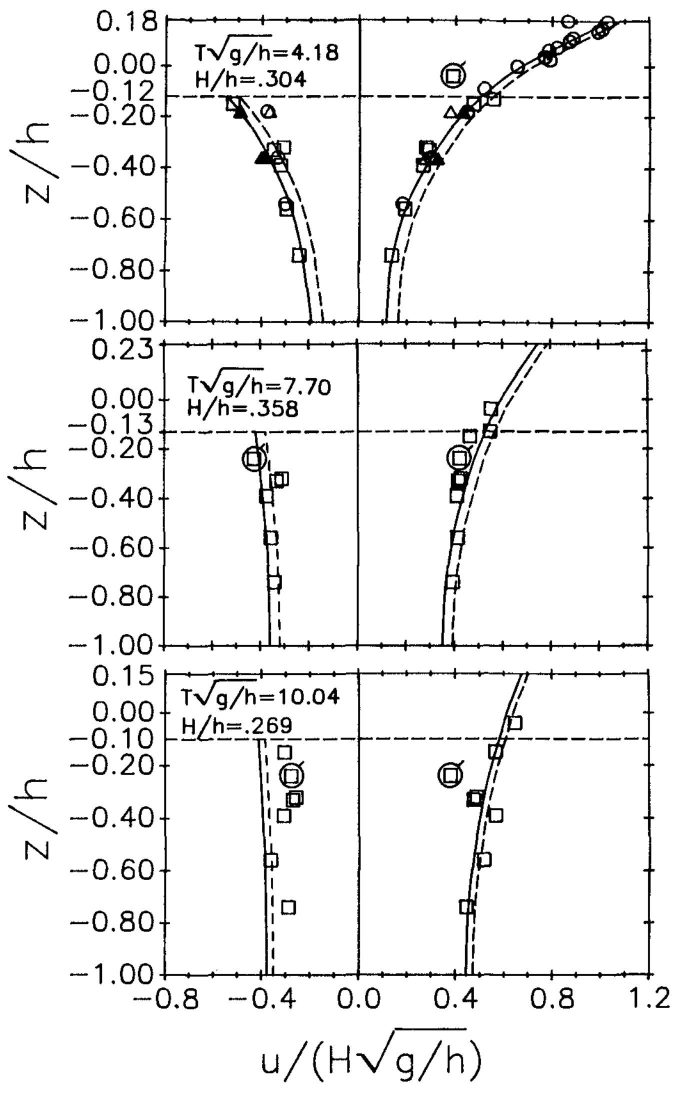

Figure 3: Nondimensional horizontal velocity under the wave crest and trough vs. relative depth. Figures 4a, b, and c show the results of Ramsden (□) electromagnetic current meters, (———) stream function theory, (- - - -) stream function theory with return flow theory, and (Ⓞ) questionable measurements. Figure 4a also shows the measurements of Jensen (1978) (o) propellor meter and Kobune (1978) (▲) hot film anemometer, (△) propellor meter.

5% to 10% for the 2.5 sec. to 6. sec. waves, respectively. The free waves may be about as large as the second order Stokes wave as shown by Buhr Hansen and Svendsen (1974). The data of this study and that of Bullock and Short (1985) showed that the amplitude of the second harmonic of η is typically 10%, and at most 25%, of the fundamental harmonic. The second harmonics of 25% most likely include a contribution from both the free wave and the Stokes wave. Thus, the free wave is probably at most 12% of the Stokes first harmonic. Since the free and reflected waves travel in opposite directions, their effect on the horizontal velocity will be the largest where the crest of one coincides with the trough of the other. With a reflection of 10% and a free wave of 12% this effect should be limited to $\pm 22\%$ of the Stokes first harmonic. To correct the theory for the reflection and the free wave, one must know their amplitude as well as their phase relative to the Stokes wave.

Since the free wave celerity is smaller than the Stokes wave celerity, one can compute the time lag between the leading edge of the two wave groups for any location along the flume. For station 1 the lag between the groups is 7.5 and .9 Stokes wave periods for the 2.5 sec. and 6. sec. waves, repectively. Since the measured velocities plotted in Fig. 3 are from about the fourth wave, the results in Fig. 3a from this study were most likely obtained before arrival of the free wave. Since the free waves have not arrived and the reflections are about 5%, the agreement between measurements and predictions is very close. As the wave length increases one should expect more variability in the measurements, due to the free and reflected waves, as shown in Figures 3b and 3c.

In Fig. 3a the ratio of the return flow to the maximum velocity increases with increasing depth due to the attenuation of the water wave velocity. As a result, the return flow reaches 26% of the maximum measured velocity at a relative depth of $z/h = -.74$. From all the measurements in this study, the stream function theory modified for the return flow predicted the maximum measured velocities within $\pm 15\%$ during 85% of the runs. A few measurements were from 30% to 50% less than predicted, however most of these were associated with questionable current meter response.

The mean wave profile ($\overline{\eta}$) and the return flow ($\overline{u}$) are shown for the largest 2.5 sec. wave and 5.3 sec. wave in Figures 4a and 4b, respectively. The mean values were computed at specific points in

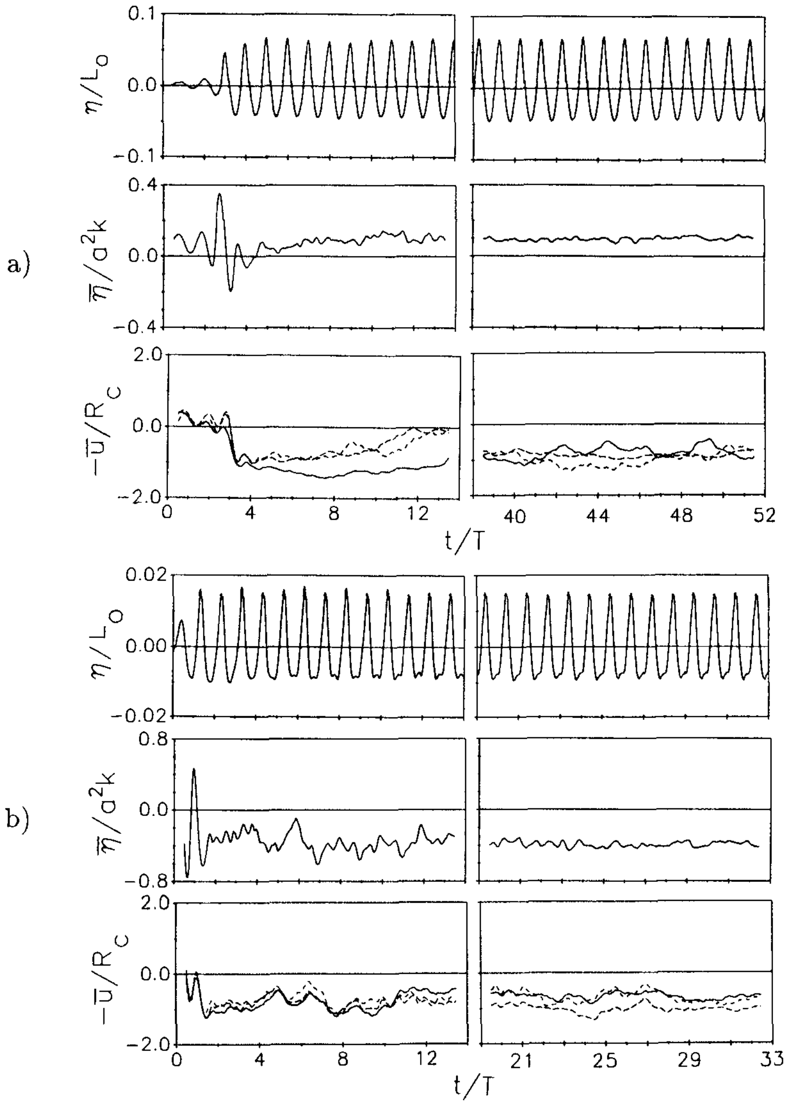

Figure 4: Nondimensional water surface profile, mean water surface, and return flow vs. time. Wave conditions: (a) T=2.5 sec. ($T\sqrt{g/h}$ = 4.18), H=1.07 m. (H/h = .304); and (b) T=5.3 sec. ($T\sqrt{g/h}$ = 8.87), H=1.07 m. For $-\overline{u}/R_c$ the various lines correspond to (——) $z/h = -.74$, (– – –) $z/h = -.33$, and (- - - -) $z/h = -.32$.

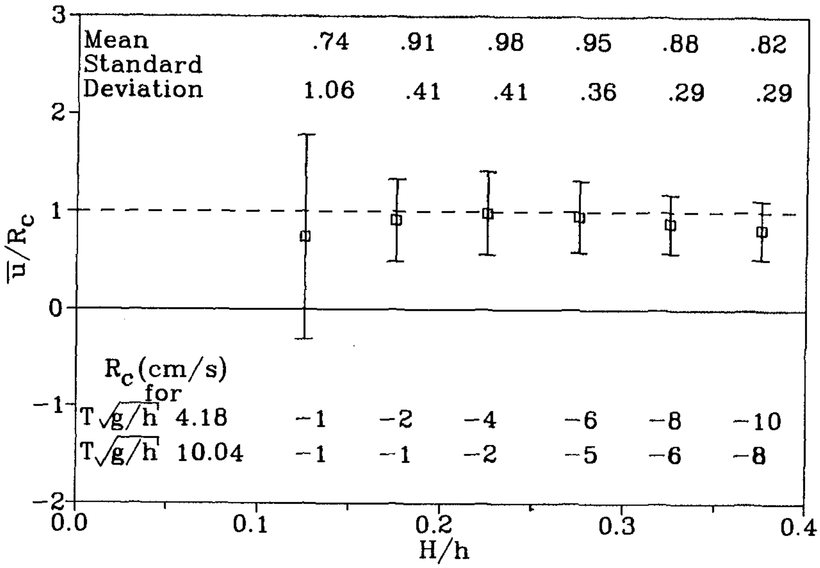

Figure 5: Mean and standard deviation of the normalized return flow vs. the relative wave height for all the runs. In the bottom of the figure the theoretical return flow is shown at each wave height for the 2.5 sec. and 6. sec. waves.

time by averaging the record over a wave period which is centered at that point. This average is then computed at 32 points per wave period over the entire record. The water surface profile is shown on the top of each figure and the time scale is reference to the start of the measurements. The break in the time scale represents the amount of time elapsed between the two blocks of data.

For the nearly deep water wave (Fig. 4a), the return flow at relative depths of −.33 and −.32 show a gradual rize to zero during the first data block, while settling to nearly constant values in the second block. This was characteristic of the 2.5, 3.7, and 4.6 sec. waves, although the unsteadiness in the first data block was quite variable from one run to another. Figure 4b is characteristic of the 5.3 and 6. sec. waves, where the return flow is fairly stable from the start except for a subharmonic response which may be due to long waves excited at these wave periods.

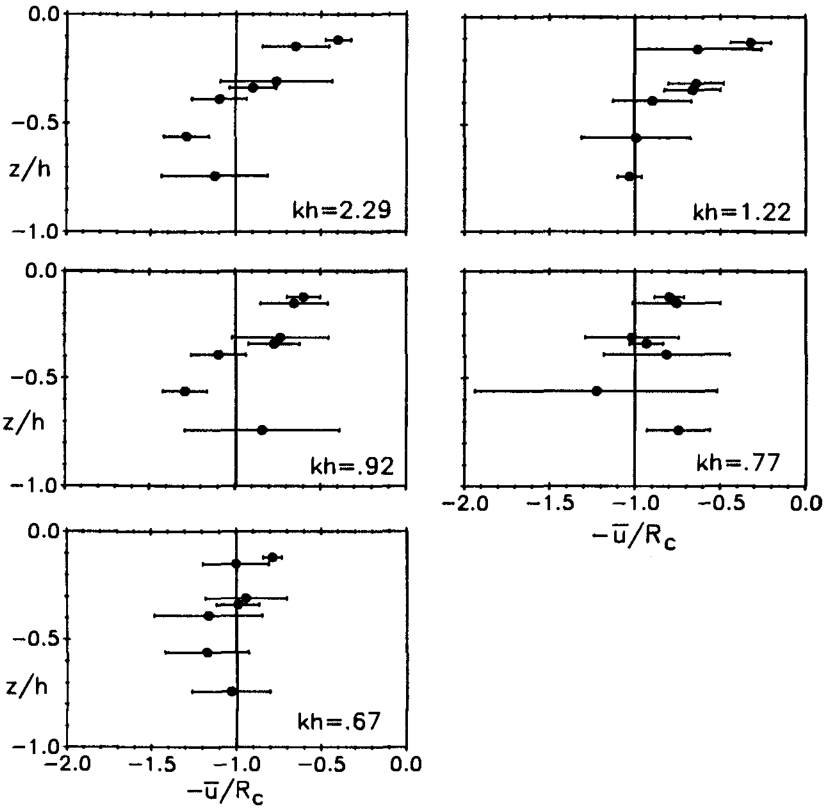

Figure 6: Mean and standard deviation of the nondimensional return flow, averaged over the wave height, vs. the relative depth for each wave period.

Surprisingly, $\overline{\eta}$ was positive for all the 2.5 second waves (Fig. 4a) and the smallest 3.7 sec. wave. For all the other wave conditions (Fig. 4b) $\overline{\eta}$ was negative in accordance with the theory of Brevik (1979) which always predicts a negative $\overline{\eta}$. For the shorter waves, $\overline{\eta}$ tended to stabilize much more rapidly and had no large jumps like that in (Fig. 4b) at t/T=5 which were characteristic of the longer waves records. In Figure 4b the η record shows the time lag between the free and Stokes waves, since the hump in the wave

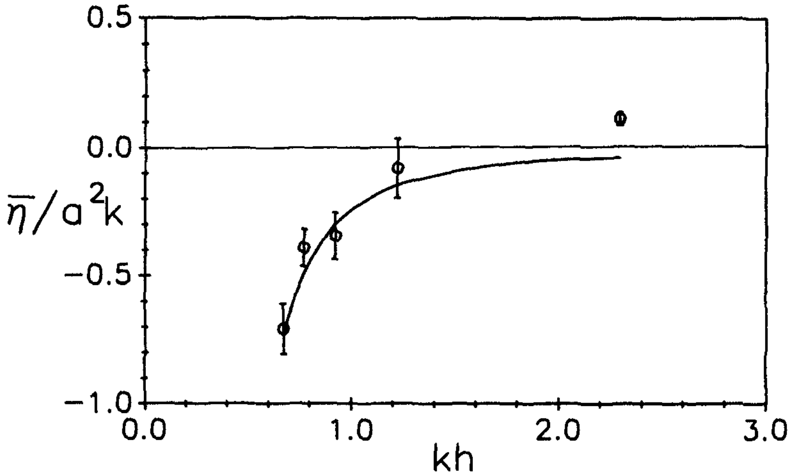

Figure 7: Mean water surface set-down vs. kh. The mean and standard deviation of the measurements are compared with the theory of Brevik (1979) which is shown as a solid line.

trough takes a few wave periods to develope.

Figure 5 shows $\overline{u}/R_c$ vs. the relative wave height for all the runs. The data were grouped according to the wave period. The measured horizontal velocity was averaged over eight waves to compute $\overline{u}$. The average was started at about the third wave of constant height. This figure shows that on the average, Kim's theory predicts the return flows within about 18%. The smallest return flows had large variability which may be due to the numerical sensitivity of dividing two small numbers, and it may indicate a lower limit of the current meters sensitivity.

The values of $-\overline{u}/R_c$, averaged over the wave heights at each vertical location are shown for each wave period in Figure 6. The measured return flow was computed as in Figure 5. There is considerable vertical structure to the return flow which tends to diminish as the wave period increases. Due to this structure, Kim's theory overpredicts the return flow above $z/h = -.4$, while it tends to underpredict the return flow below this level. It may be that if one could extend this trend, the return flow would become zero somewhere near the mean water surface and would be positive above that point, becoming zero again at the wave crest elevation.

Figure 7 shows the normalized wave set-down plotted against kh. The mean water surface elevations were computed by averaging the last eight waves of the first 14 wave period data block. The measurements follow Brevik's (1979) theory closely for the longer waves, but as the wave length becomes smaller his theory tends to zero while the measurements show a wave set-up.

CONCLUSIONS

There is a return flow under large amplitude waves. For the conditions of this study Kim's theory is a good first approximation except very near the mean water surface. Including Kim's return flow model with stream function wave theory improves the agreement between the measured and predicted velocities. The return flow is a function of time and depth. Brevik's theory predicts the water surface set-down closely except for the nearly deep water waves. No dependence of the return flow or the water surface set-down with horizontal position could be determined from these data.

REFERENCES

Brevik, I. (1979). "Remarks on set-down for wave groups and wave-current systems." *Coastal Engrg.*, 2, 313-326.

Bullock, G.N., and Short, I. (1985). "Water particle velocities in regular waves." *J. of Waterway, Port, Coastal and Ocean Div.*, ASCE, 111(02), 189-200.

Buhr Hansen, J., and Svendsen, Ib A. (1974). "Laboratory generation of waves of constant form." *Proc. 14th Conf. Coastal Engrg.*, 1, 321-339.

Chandler, B.D., and Hinwood, J.B. (1982). "Combined wave-current forces on horizontal cylinders." *Proc. 18th Conf. Coastal Engrg.*, 3, 2171-2188.

Dalrymple, R.A. (1976). "Wave-induced mass transport in water waves." *J. of Waterway, Port, Coastal and Ocean Div.*, ASCE, 102(02), 255-264.

Jensen, R.E. (1978). "Finite amplitude deep water waves: a comparison of theoretical and experimental kinematics and dynamics." Masters Thesis, Department of Civil Engineering, Oregon State University, Corvallis, OR, U.S.A.

Kim, T.I. (1984). "Mass transport in laboratory water wave flumes." Doctoral Thesis, Department of Civil Engineering, Oregon State University, Corvallis, OR, U.S.A.

Kim, T.I., Hudspeth, R.T., and Sulisz, W. (1986). "Ciculation kinematics in nonlinear laboratory waves." *Proc. 20th Conf. Coastal Engrg.*, 1, 381-395.

Kobune, K. (1978). "Random wave velocity field from periodic theory." Masters Thesis, Department of Civil Engineering, Oregon State University, Corvallis, OR, U.S.A.

Longuet-Higgins, M.S. (1953). "Mass transport in water waves." *Philosophical Transactions of the Royal Society of London*, Series A, 245(903),535-581.

Longuet-Higgins, M.S., and Stewart, R.W. (1964). 'Radiation stresses in water waves; a physical discussion, with applications." *Deep-Sea Research*, 11, 529-562.

Nath, J.H., (1978). "Drift speed of bouys in waves." *Proc. 16th Conf. Coastal Engrg.*, 3, 859-873.

Ramsden, J.D. (1987). "Kinematics and return flow in a closed wave flume." Masters Thesis, Department of Civil Engineering, Oregon State University, Corvallis, OR, U.S.A.

Russell, R.C.H., and Osorio, J.D.C. (1958). "An experimental investigation of drift profiles in a closed channel." *Proc. 6th Conf. Coastal Engrg.*, Council on Wave Research, ASCE, 171-193.

Stokes, G.G. (1847). "On the theory of oscillatory waves." *Transactions of the Camridge Philosophical Society*, London, England, 8:441-455.